Internal Cooling in a Semiconductor Laser Diode

K. P. Pipe, R. J. Ram, and A. Shakouri

***Abstract*—A thermal model of a diode laser structure is developed which includes a bipolar thermoelectric term not included in previous models. It is shown that heterostructure band offsets can be chosen so that there are thermoelectric cooling sources near the active region; this method of cooling is internal to the device itself, as opposed to temperature stabilization schemes which employ an external cooler. A novel laser structure is proposed that is capable of internal cooling in the $Ga_{1-x}In_xAs_ySb_{1-y}$–GaSb material system with $\lambda = 2.64$ μm.**

***Index Terms*—Electrothermal effects, lasers, laser thermal factors, photothermal effects, semiconductor lasers, thermionic emission, thermionic energy conversion, thermoelectric devices, thermoelectric energy conversion, thermoelectricity.**

I. Introduction

HEAT MANAGEMENT can be a critical issue in diode laser design, due to the strong temperature dependencies of threshold current, quantum efficiency, and device lifetime [1], [2]. Existing methods for temperature stabilization typically involve placing an external Peltier cooler in the vicinity of the device, either by mounting the device on a heat sink or by fabricating a surface cooler [3]. An approach amenable to integration has been developed recently by [4]. By taking advantage of thermionic and thermoelectric effects in III–V heterostructures, cooling power densities of several hundred W/cm^2 have been obtained in micrometer-thick films. These unipolar heterostructure coolers have been used in a monolithic (though external) manner to stabilize the temperature of nearby devices; the interfaces of the cooler sink the heat that is produced by the device which is grown above [5].

Here, we apply the concept of heterostructure integrated cooling to examine heat transport that is internal to the device itself. Instead of fabricating a heat-producing device on top of a cooling layer structure, we modify the device itself (in this case, a laser diode) such that every interface within the device provides thermoelectric cooling and the associated thermoelectric heating is mostly transferred to locations near the heat sinks. In doing so, we take into account Joule heating, contact resistance, and nonradiative recombination, as well as a bipolar thermoelectric term which has been neglected in previous thermal models [6], [7].

Manuscript received October 22, 2001. A. Shakouri was supported by the National Science Foundation (NSF) under the CAREER program.

K. P. Pipe and R. J. Ram are with Research Laboratory of Electronics, Massachusetts Institute of Technology, Cambridge, MA 02139 USA.

A. Shakouri is with the Jack Baskin School of Engineering, University of California, Santa Cruz, CA 95064-1077 USA.

Publisher Item Identifier S 1041-1135(02)01857-8.

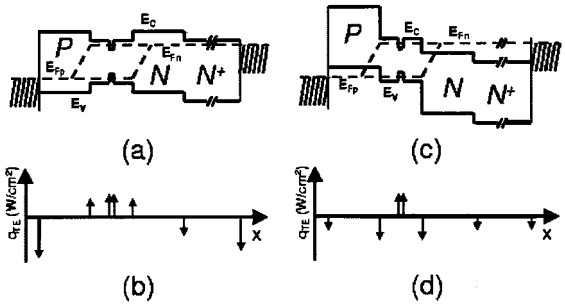

Fig. 1. Band structure and thermoelectric heat source distribution for (a) and (b) conventional SCH, and (c) and (d) ICICLE.

II. Thermoelectric Model

In the design of a semiconductor laser, it is desirable to have both the optical mode and the carriers confined to the active region in order to produce the greatest overlap between the mode and the gain medium. This is accomplished in the traditional double-heterostructure device by using a core material which has a smaller bandgap than the adjacent cladding regions, since for most material systems refractive index has an inverse relationship with bandgap [7]. Carrier confinement is simultaneously realized since the heterointerfaces between most III–V materials are Type-I. Additional carrier confinement is achieved in a separate-confinement heterostructure (SCH) device by adding a quantum well (QW) to the waveguide core, as shown in Fig. 1(a).

Using a heterostructure for confinement allows control of the electronic density-of-states, and hence the energy levels occupied by the carriers that contribute to the injection current. In the degenerate case for electrons, defined by a Fermi–Dirac distribution $f_{\rm eq}$ with quasi-Fermi energy E_{Fn} deep within the conduction band, the electrons that participate in conduction are nearly symmetrically distributed about E_{Fn} in a region of width kT within the "Fermi window" $(-(\partial f_{eq}/\partial E))$. The average carrier transport energy with respect to the quasi-Fermi energy is given by

$$\overline{E_{\rm tr}} = \frac{\int \sigma(E)(E - E_{Fn})\left(-\dfrac{\partial f_{\rm eq}}{\partial E}\right)dE}{\int \sigma(E)\left(-\dfrac{\partial f_{\rm eq}}{\partial E}\right)dE} \tag{1}$$

where the "differential" conductivity $\sigma(E)$ gives the contribution of a carrier at energy E to the overall conductivity [8].

As carriers flow between quasi-equilibrium distributions on either side of a heterojunction, they exchange an amount of heat energy equal to $\Delta\overline{E_{\rm tr}}$ with the surrounding lattice. This process is described in thermoelectric terms by the Peltier coefficient, which is given by $\Pi = \overline{E_{\rm tr}}/q$. The total thermoelectric heat

exchange Q at the junction is then written in terms of the current I, and the difference in Peltier coefficients across the junction $\Delta\Pi$ as $Q = I^*\Delta\Pi$.

One should note that Peltier heat exchange is a thermodynamically reversible process (as opposed to Joule heating); either cooling or heating can be produced depending on the direction of the current. An approximate Peltier coefficient can be defined for each layer in a device by averaging the coefficient over the thickness of the layer. The approximate thermoelectric heat distribution can then be given as interface delta function sources with magnitudes given by $I^*\Delta\Pi$. This bulk equilibrium approximation does not take into account the finite energy relaxation length of carriers, and hence is best applied to thick layers and small electric fields; nonequilibrium and junction effects such as thermionic emission and thermal boundary impedances are likewise neglected. In unipolar heterostructure coolers, thermionic cooling can be tailored such that it produces cooling on the same order as thermoelectric cooling [9].

Given this model for approximating the Peltier coefficient of a given layer, it is possible to examine a typical SCH laser diode in terms of thermoelectric heat exchange. Shown in Fig. 1(a) is an SCH device, with ohmic contacts and n^+ substrate, biased approximately at threshold. Since electrons and holes have separate quasi-Fermi energies, one can define Peltier heat exchange terms for each type of carrier at the heterointerfaces and then add them together to yield the total bipolar thermoelectric heat source distribution. As the carriers enter the core region, their average transport energy is reduced, causing heat to be generated at the cladding/core interfaces. A portion of the injected carriers leak out of the core region without recombining, giving rise to thermoelectric cooling at the second core/cladding interface. Since the injection current is typically much larger than the leakage current, however, the core/cladding junctions will exhibit an overall positive heat flux as shown in Fig. 1(b). In the case of appreciable leakage current, less thermoelectric heating is expected, although this comes at the expense of the laser's quantum efficiency [10].

A similar argument can be used to estimate thermoelectric cooling or heating at the QW interfaces. However, the nonequilibrium nature of the carrier distribution in the well should be taken into account [11]. In the following discussion, however, these effects are ignored; we will keep the QW heat exchange terms the same for the various designs so that small errors in the calculation of QW heating will not change the validity of the analysis. Notice that there is a variation of the quasi-Fermi levels in the cladding regions. This corresponds to a position-dependent Peltier coefficient, since the average energy of moving carriers is changing. We have included this in the calculations by using an average Peltier coefficient at interfaces as discussed above. Below threshold, the strong built-in electric field in the undoped core causes a variation in $\overline{E_{\rm tr}}$, again necessitating averaging as well as giving bipolar Peltier heat exchange terms which can change sign as a function of bias due to the dependence of the Peltier coefficient on carrier density [12].

Heating in the active region spreads out the carrier distribution in energy, leading to an exponentially higher threshold current [7]. Thermoelectric heat exchange, as well as terms not shown in Fig. 1(b) such as Joule heating, contact resistance heating, and nonradiative recombination, all contribute to decreased laser performance in the typical SCH design. Often the relative magnitude of the active region thermoelectric terms is small, producing only a slight predicted increase in laser temperature for a typical SCH design [13]. By modifying the band structure, however, one can construct a device whose thermoelectric heat exchange distribution includes sizable cooling terms in the vicinity of the core.

III. ICICLE Structure

Fig. 1(c) depicts the band structure of such a device. In this case, injection current and leakage current both contribute to cooling at the cladding/core interfaces, as shown in Fig. 1(d). Because the same carriers which eventually radiatively recombine also produce cooling, this configuration is termed an injection current internally cooled light emitter (ICICLE). The electrical resistance of the ICICLE structure will be nearly the same as the traditional SCH design as long as the barrier heights are small enough to restrict electron transport to the diffusive rather than the thermionic regime. It is important to note that the sums of the thermoelectric heat exchange terms for the ICICLE design and for the traditional SCH design are nearly the same for the same bias.

There are two ways by which the optimization of thermoelectric effects within the ICICLE design can improve the temperature characteristics of a semiconductor laser. First of all, the spatial distribution of Peltier cooling and heating terms at the interfaces is modified so that cooling happens near the active region and the complementary heating occurs at the device edges, where it is more readily conducted away. Secondly, the design can be such that the sum of the Peltier cooling and heating terms produce a net cooling in the device. This can be viewed as an extension of previous work aimed at cooling a p-n diode through radiative recombination at energy levels higher than $qV_{\rm Bias}$ [14]–[16]. When the ICICLE is biased below threshold ($qV_{\rm th} \approx \hbar\omega$ is approximately the QW bandgap), thermal injection of carriers from the cladding layers leads to additional light emission at $\hbar\omega$. Above threshold, spontaneous emission becomes fixed, clamping the entropy path out of the device and limiting additional optical refrigeration.

Two ways to obtain the "staircase" ICICLE structure are to dope the cladding regions heavily or to use a material system whose alignment is Type-II. Heavy p-type doping usually leads to excessive intervalence band absorption, so it is preferable to use a Type-II interface at the p-cladding/core interface. The n-cladding/core interface can typically be pulled into correct alignment by heavy n-type doping. A Type-II interface may also be used at this interface, as long as the n-cladding bandgap remains larger than that of the core.

IV. Antimonide ICICLE

Conventional SCH and ICICLE structures in the $Ga_{1-x}In_xAs_ySb_{1-y}$ material system at the same current bias are depicted along with their associated bipolar thermoelectric heat exchange terms in Fig. 2. The modeling of these example structures was not performed self-consistently (taking into account electrical, optical, and thermal effects), but is

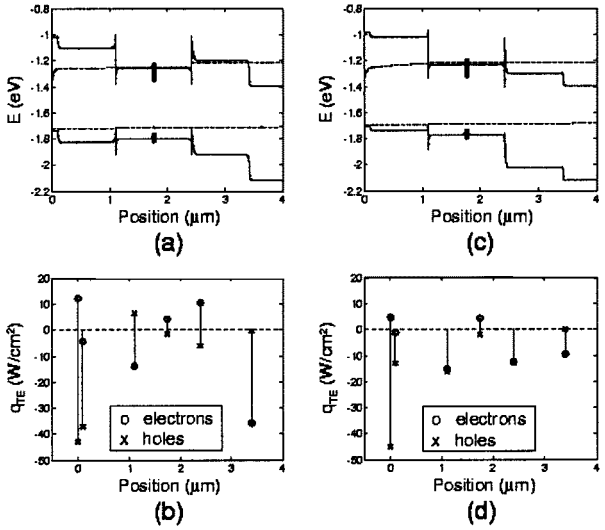

Fig. 2. Band structure and bipolar thermoelectric heat source distribution for GaInAsSb (a) and (b) conventional SCH, and (c) and (d) ICICLE structures at a current density of 475 A/cm^2. Contact/substrate term is not shown.

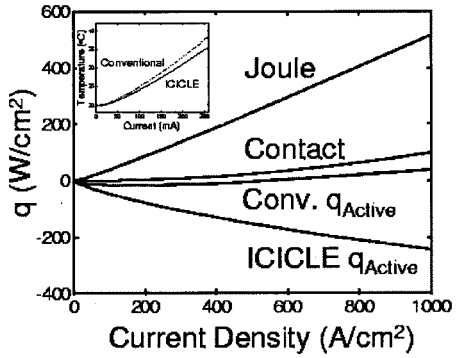

Fig. 3. Heat source terms for GaInAsSb conventional SCH and ICICLE structures. Inset: Calculated QW temperature.

intended to demonstrate an application of the concepts outlined above to a laser structure below threshold. Carrier transport was calculated by solving the drift-diffusion equations self-consistently with Poisson's equation [17]. The Type-II interface of GaInAsSb was used to decrease the doping level required to pull the p-cladding into ICICLE alignment. Each structure shown in Fig. 2 is comprised of a p$^+$ GaSb cap doped at 3×10^{18}, GaSb cladding layers, an undoped $Ga_{0.8}In_{0.2}As_{0.17}Sb_{0.83}$ core, and several $\lambda = 2.64$-μm $Ga_{0.7}In_{0.3}As_{0.26}Sb_{0.74}$ QWs, on an n$^+$ GaSb substrate doped at 3×10^{18}. QWs can be achieved in this material system by using either a "W" alignment (as done here) or by adding strain. The n-type and p-type cladding layers of the conventional SCH structure are both lightly doped at 1×10^{17}, whereas the cladding layers of the ICICLE are more heavily doped at 1×10^{18}. Leakage currents at threshold are approximately 4% at 190 A/cm^2 in the conventional SCH structure and 2% at 380 A/cm^2 in the ICICLE structure. Notice that cooling caused by electron leakage out of the core in the conventional structure overcomes the injection heating term at the p-cladding/core interface. Further modeling confirmed that the structures are single-mode and have an optical mode overlap of 0.4% per QW. These characteristics are typical for lasers in this material system, which can have threshold current densities as low as 50 A/cm^2 [18].

The actual temperature distributions for the two configurations are geometry dependent, but the difference in active region temperature is mostly due to the difference in nearby thermoelectric heat exchange terms. Fig. 3 plots the sum of the cladding/core and core/QW terms as a function of current bias, along with terms for Joule heating and contact resistance heating (assuming $R_{\rm cont} \approx 10^{-7}\ \Omega{\cdot}{\rm cm}^2$, which is small due to Fermi-level pinning in contacts to p-GaSb). To illustrate the effects of heat source placement in the two structures, the QW temperature was simulated for a 500 μm $\times$ 50 μm structure using a two-dimensional finite-element model.

In summary, by modifying the conventional SCH laser design to shift internal thermoelectric cooling to the active region, device overheating can be reduced and eventually temperature stabilization can be achieved in a way that is quite different from methods which utilize an external cooler.

REFERENCES

[1] H. J. Yi, J. Diaz, I. Eliashevich, M. Stanton, M. Erdtmann, X. He, L. J. Wang, and M. Razeghi, "Temperature dependence of threshold current density $J_{\rm th}$ and differential efficiency η_d of high-power InGaAsP/GaAs $\lambda = 0.8\mu$m lasers," *Appl. Phys. Lett.*, vol. 66, p. 253, 1995.

[2] U. Menzel, A. Bärwolff, P. Enders, D. Ackermann, R. Puchert, and M. Voss, "Modelling the temperature dependence of threshold current, external differential efficiency and lasing wavelength in QW laser diodes," *Semicond. Sci. Technol.*, vol. 10, p. 1382, 1995.

[3] P. R. Berger, N. K. Dutta, K. D. Choquette, G. Hasnain, and N. Chand, "Monolithically Peltier-cooled vertical-cavity surface-emitting lasers," *Appl. Phys. Lett.*, vol. 59, p. 117, 1991.

[4] A. Shakouri and J. E. Bowers, "Heterostructure integrated thermionic coolers," *Appl. Phys. Lett.*, vol. 71, p. 1234, 1997.

[5] C. LaBounty, A. Shakouri, P. Abraham, and J. E. Bowers, "Monolithic integration of thin film coolers with optoelectronic devices," *Opt. Eng.*, vol. 39, p. 2847, 2000.

[6] G. L. Tan, N. Bewtra, K. Lee, and J. M. Xu, "A two-dimensional non-isothermal finite element simulation of laser diodes," *IEEE J. Quantum Electron.*, vol. 29, p. 822, Mar. 1993.

[7] L. A. Coldren and S. W. Corzine, *Diode Lasers and Photonic Integrated Circuits*: Wiley & Sons, 1995, pp. 56–59.

[8] D. M. Rowe, *CRC Handbook of Thermoelectrics*. Boca Raton, FL: CRC Press, 1995.

[9] A. Shakouri, C. LaBounty, P. Abraham, J. Piprek, and J. E. Bowers, "Thermoelectric Effects in Submicron Heterostructure Barriers," *Microscale Thermophysical Eng.*, vol. 2, p. 37, 1998.

[10] I. Umebu, "A proposal of a method for analysing the leakage characteristics of 1.3 mm semiconductor buried heterostructure lasers," *Semicond. Sci. Technol.*, vol. 8, p. 63, 1993.

[11] G. A. Baraff, "Semiclassical description of electron transport in semiconductor quantum-well devices," *Phys. Rev. B*, vol. 55, p. 10 745, 1997.

[12] K. P. Pipe, R. J. Ram, and A. Shakouri, "Bias-dependent Peltier coefficient in bipolar devices," in *International Mechanical Engineering Congress and Exposition*, New York, Nov. 2001.

[13] ——, "Internal thermoelectric heating and cooling in heterostructure diode lasers," in *Conf. Lasers and Electro-Optics*, Baltimore, MD, May 2001.

[14] G. C. Dousmanis, C. W. Mueller, H. Nelson, and K. G. Petzinger, "Evidence of Refrigerating Action by Means of Photon Emission in Semiconductor Diodes," *Phys. Rev.*, vol. 133, p. A316, 1964.

[15] W. Nakwaski, "Optical refrigeration in light-emitting diodes," *Electron Technol.*, vol. 13, p. 61, 1982.

[16] H. Gauck, T. H. Gfroerer, M. J. Renn, E. A. Cornell, and K. A. Bertness, "External radiative quantum efficiency of 96% from a GaAs/GaInP heterostructure," *Appl. Phys. A*, vol. 64, p. 143, 1997.

[17] D. Winston, R. Hayes, and H. Fardi. SimWindows v. 1.5.0. [Online]. Available: http://www-ocs.colorado.edu/SimWindows/simwin.html.

[18] G. W. Turner, H. K. Choi, and M. J. Manfra, "Ultralow-threshold (50 A/cm^2) strained single-quantum–well GaInAsSb/AlGaAsSb lasers emitting at 2.05 μm," *Appl. Phys. Lett.*, vol. 72, p. 876, 1998.